Original Article

Necroptosis-related lncRNAs: biomarkers for predicting prognosis and immune response in lung adenocarcinoma

Chunxuan Lin[1#], Kunpeng Lin[2#], Xiaochun Lin[3#], Hai Yuan[4], Yingying Zhang[5], Zhijun Xie[6], Yong Dai[1], Luhao Liu[7#], Yoshihisa Shimada[8], Taichiro Goto[9], Katsuhiro Okuda[10], Taisheng Liu[5,11]^, Chenggong Wei[1]

[1]Department of Respiratory Medicine, Guangdong Provincial Hospital of Integrated Traditional Chinese and Western Medicine, Foshan, China; [2]Department of Abdominal Oncosurgery, Guangzhou Institute of Cancer Research, the Affiliated Cancer Hospital, Guangzhou Medical University, Guangzhou, China; [3]Department of Medical Examination Center, Guangzhou First People's Hospital, Guangzhou Medical University, Guangzhou, China; [4]Department of Cardio-Thoracic Surgery, Guangzhou Hospital of Integrated Chinese and Western Medicine, Guangzhou, China; [5]Department of Thoracic Surgery, Guangzhou Institute of Cancer Research, the Affiliated Cancer Hospital, Guangzhou Medical University, Guangzhou, China; [6]Departtment of Radiology, The Second People's Hospital of Jiangmen, Jiangmen, China; [7]Department of Organ Transplantation, The Second Affiliated Hospital of Guangzhou Medical University, Guangzhou, China; [8]Department of Thoracic Surgery, Tokyo Medical University, Tokyo, Japan; [9]Lung Cancer and Respiratory Disease Center, Yamanashi Central Hospital, Yamanashi, Japan; [10]Department of Thoracic and Pediatric Surgery, Nagoya City University Graduated School of Medical Sciences, Nagoya, Japan; [11]Department of Thoracic Surgery, Nanfang Hospital, Southern Medical University, Guangzhou, China

Contributions: (I) Conception and design: T Liu, C Wei; (II) Administrative support: C Wei; (III) Provision of study materials or patients: C Lin, L Liu, K Lin; (IV) Collection and assembly of data: X Lin, H Yuan; (V) Data analysis and interpretation: Y Zhang, X Lin, Z Xie, Y Dai, H Yuan, T Liu, C Wei; (VI) Manuscript writing: All authors; (VII) Final approval of manuscript: All authors.

[#]These authors contributed equally to this work.

Correspondence to: Chenggong Wei, MM. Department of Respiratory Medicine, Guangdong Provincial Hospital of Integrated Traditional Chinese and Western Medicine, No. 16, Nanwu Road, Guicheng, Nanhai District, Foshan 528200, China. Email: wcg368@126.com; Taisheng Liu, MD. Department of Thoracic Surgery, Guangzhou Institute of Cancer Research, the Affiliated Cancer Hospital, Guangzhou Medical University, Guangzhou, China; Department of Thoracic Surgery, Nanfang Hospital, Southern Medical University, No. 78 Hengzhi Gang, Yuexiu District, Guangzhou 510095, China. Email: liutaisheng2009@163.com.

Background: Lung adenocarcinoma (LUAD) is one of the most prevalent types of lung cancer (LC), accounting for 50% of all LC cases. Despite therapeutic advancements, patients suffer from adverse drug reactions. Furthermore, the prognosis of LC patients remains poor. Necroptosis is a novel mode of cell death and is critically involved in regulating immunotherapy in patients. However, the correlation between the necroptosis-related long non-coding RNA (lncRNA) (necro-related lnc) signature (NecroLncSig) and the response of patients with LUAD to immunotherapy is unclear. This study developed a model using lncRNAs to predict the prognosis of patients with LUAD.

Methods: We obtained the transcriptomic and clinical data of LUAD patients from The Cancer Genome Atlas (TCGA) database. Next, we conducted a co-expression analysis to identify the necro-related lnc. In addition, we constructed the NecroLncSig using univariate and least absolute shrinkage and selection operator (LASSO) Cox regression analyses. Then we evaluated and validated the NecroLncSig using a Kaplan-Meier (KM) survival analysis, receiver operating characteristic (ROC) curves, principal component analysis (PCA), Gene Ontology (GO) enrichment analysis, a nomogram, and calibration curves. Finally, we used the NecroLncSig to predict the responses of patients to immunotherapy.

Results: We constructed the NecroLncSig based on seven necro-related lnc. The patients were classified into a high-risk group (HRG) and a low-risk group (LRG). The overall survival (OS) of patients in the HRG was significantly poorer in the training, testing, and entire sets (P<0.05) than that of the patients in the LRG. Univariate and multivariate Cox regression analyses demonstrated that the risk score could predict

^ ORCID: 0000-0002-0132-4707.

the OS of patients in an independent manner (P<0.001). Time-dependent ROC analysis demonstrated that the area under the curve values of the NecroLncSig for 1-, 2-, and 3-year OS were 0.689, 0.700, and 0.685, respectively, for the entire set. Furthermore, the Tumor Immune Dysfunction and Exclusion (TIDE) algorithm showed that the response of patients in the HRG to immunotherapy was better than that of patients in the LRG.

Conclusions: Necro-related lnc can affect disease progression and patient prognosis. In addition, these lncRNAs can be used to design therapeutic strategies, such as immunotherapy, to treat patients with LUAD.

Keywords: Lung adenocarcinoma (LUAD); necroptosis; long non-coding RNA (lncRNA); overall survival (OS)

Submitted Jul 19, 2024. Accepted for publication Sep 25, 2024. Published online Oct 28, 2024.
doi: 10.21037/tlcr-24-627
View this article at: https://dx.doi.org/10.21037/tlcr-24-627

Introduction

Lung cancer (LC) is the major cause of cancer-related deaths worldwide (1). Lung adenocarcinoma (LUAD) is one of the most prevalent subtypes of LC (2). Advancements in therapeutic approaches, such as surgery, radiotherapy, molecular therapy, and immunotherapy, have improved the clinical outcomes of patients with LUAD (3-6). However, despite these advancements, LUAD remains one of the most aggressive, rapidly progressing, and fatal types of tumors. The overall survival (OS) of patients with LUAD is <5 years (2,7,8). Therapeutic strategies for treating patients with LUAD, including conventional chemotherapy and target therapy, have frequent side effects and poor success rates. Therefore, the identification of biomarkers to predict the immune response and prognosis of patients with LUAD is of great significance.

Necroptosis is a novel mode of programmed necrotic cell death. It is regulated by receptor-interacting protein 1/3 (RIP1/3) and mixed lineage kinase domain-like protein (MLKL) (9-12). Studies have shown that necroptosis is significantly involved in the occurrence, development, metastasis, and immune responses of cancers (13-15). RIPK1- and RIPK3-dependent necroptosis downstream of tumor necrosis factor receptor-1 mediates the oligomerization and transportation of MLKL to the cell membrane, causing cell expansion and ultimately cell death (16). Furthermore, necroptosis is an inflammatory form of cell death. Hence, it can induce a proinflammatory tumor microenvironment (TME), thus promoting the malignant transformation of cells and cancer progression (17).

Long non-coding RNAs (lncRNAs) are a type of RNA more than 200 nucleotides in length (18). Mounting evidence suggests that lncRNAs regulate gene expression at the chromatin, transcriptional, and posttranscriptional levels (19-21). The lncRNA protein P53 (TP53)-regulated inhibitor of necrosis under glucose starvation protects tumor cells from necroptosis by inhibiting the thrombin receptor agonist peptide/glycogen synthase kinase 3 beta/nuclear factor kappa B signaling pathway (22). In hepatocellular carcinoma (HCC), low LINC00176 levels induce the secretion of tumor suppressor microRNA-9 (miR-9) and miR-185, thereby disrupting the cell cycle and inducing necroptosis (23). However, the involvement and mechanism of necroptosis-related lncRNAs (necro-related lncs) in the prognosis of patients with LUAD are unclear. Thus, designing a necroptosis-based treatment strategy is challenging.

In this study, we obtained the necro-related lnc data of patients with LUAD from The Cancer Genome Atlas (TCGA) database. First, we identified seven necro-related lncs and established a novel prognostic model for LUAD patients. Next, we performed Gene Ontology (GO) enrichment analysis to screen for the pathways enriched in patients in the high-risk group (HRG) and low-risk group (LRG). Lastly, we constructed a nomogram and plotted calibration curves to predict the OS of patients. We present this article in accordance with the TRIPOD reporting checklist (available at https://tlcr.amegroups.com/article/view/10.21037/tlcr-24-627/rc).

Methods

Acquisition of data of patients with LUAD

We obtained the transcriptome, mutation, and clinical characteristic data of patients with LUAD from TCGA (https://portal.gdc.cancer.gov/) database. We reduced the

statistical bias by eliminating the data of patients without OS data. The study was conducted in accordance with the Declaration of Helsinki (as revised in 2013).

Identification of necroptosis-related genes (NRGs) and lncRNAs

We screened the following 14 NRGs from previous studies: *CASP8*, *BIRC2*, *BIRC3*, *CYLD*, *EZH2*, *HMGB1*, *MLKL*, *NDRG2*, *PGAM5*, *RIPK1*, *RIPK3*, *TRAF2*, *USP22*, and *ZBP1* (Table S1) (24-35). By utilizing the GTF annotation files for human lncRNAs retrieved from the GENCODE website (https://www.gencodegenes.org/, accessed on September 13, 2021), a total of 14,057 lncRNAs were identified from the TCGA-LUAD RNA sequencing (RNA-seq) data. Subsequently, the Pearson correlation analysis was conducted between the lncRNAs and NRGs, applying a threshold of |Pearson R| >0.4 and P<0.001, to identify necro-related lncs. As a result, a total of 2,195 necro-related lncs were identified (table available at https://cdn.amegroups.cn/static/public/tlcr-24-627-1.xlsx).

Highlight box

Key findings

- Necroptosis-related long non-coding RNAs (necro-related lncs) could affect disease progression and patient prognosis. Further, these necro-related lncs could be used to design therapeutic strategies, such as immunotherapy for treating patients with lung adenocarcinoma (LUAD).

What is known, and what is new?

- Necroptosis is a recently identified form of cell death that plays a crucial role in modulating immunotherapy in patients.
- We developed a necro-related lnc signature (NecroLncSig) based on seven necro-associated lncs. Patients were stratified into high-risk group (HRG) and low-risk group (LRG). In the training, testing, and entire sets, patients in the HRG exhibited significantly poorer overall survival (OS) compared to those in the LRG (P<0.05). Univariate and multivariate Cox regression analyses confirmed that the risk score was an independent predictor of OS (P<0.001). Time-dependent receiver operating characteristic analysis revealed that the area under the curve values for the NecroLncSig in predicting 1-, 2-, and 3-year OS were 0.689, 0.700, and 0.685, respectively, across the entire set. Additionally, the Tumor Immune Dysfunction and Exclusion algorithm indicated that patients in the HRG had a more favorable response to immunotherapy than those in the LRG.

What is the implication, and what should change now?

- The NecroLncSig can be used to predict the survival and response of patients to immunotherapy and to screen patients with LUAD who may respond to immunotherapy with high sensitivity. Prospective studies need to be conducted in the future to validate these findings.

Establishment and validation of the necro-related lncs signature (NecroLncSig)

We divided the patients from TCGA (entire set; n=504) into training (n=252) and testing (n=252) sets. The NecroLncSig was constructed based on the training set and validated using the entire and testing sets. The clinical characteristics of the patients are shown in Table S2. There were no statistically significant differences between the clinical characteristics of the patients in these three sets (P>0.05). Of the 2,195 necro-related lncs, we identified 22 patient prognosis-associated lncRNAs using univariate Cox regression analysis (Table S3). Next, we performed least absolute shrinkage and selection operator (LASSO) Cox regression analysis of the 22 necro-related lncs. Finally, we identified seven necro-related lncs to establish the NecroLncSig. The following formula was used to calculate the risk score:

$$\begin{aligned}\text{Risk score} = {} & \text{coef}(\text{lncRNA1}) \times \text{expr}(\text{lncRNA1}) \\ & + \text{coef}(\text{lncRNA2}) \times \text{expr}(\text{lncRNA2}) \\ & + \ldots + \text{coef}(\text{lncRNAn}) \times \text{expr}(\text{lncRNAn})\end{aligned} \quad [1]$$

where "coef (lncRNAn)" represents the coefficient of the lncRNAs, and "expr (lncRNAn)" represents the expression of lncRNAs.

We classified LUAD patients in all the sets into the HRG and LRG using the median risk score as the threshold value. Next, we performed univariate and multivariate Cox regression analyses to determine the independent variable factors of the NecroLncSig. Finally, we determined the specificity and sensitivity of the NecroLncSig using receiver operating characteristic (ROC) curves.

GO enrichment analysis

We identified the differentially expressed genes (DEGs) (table available at https://cdn.amegroups.cn/static/public/tlcr-24-627-2.xlsx) between the HRG and LRG in the entire set based on the following criteria: false discovery rate <0.05 and $|\log_2\text{fold change}| > 1$. Next, we conducted GO enrichment analysis to investigate the functions of these DEGs. Functions with P values <0.05 were considered significantly enriched.

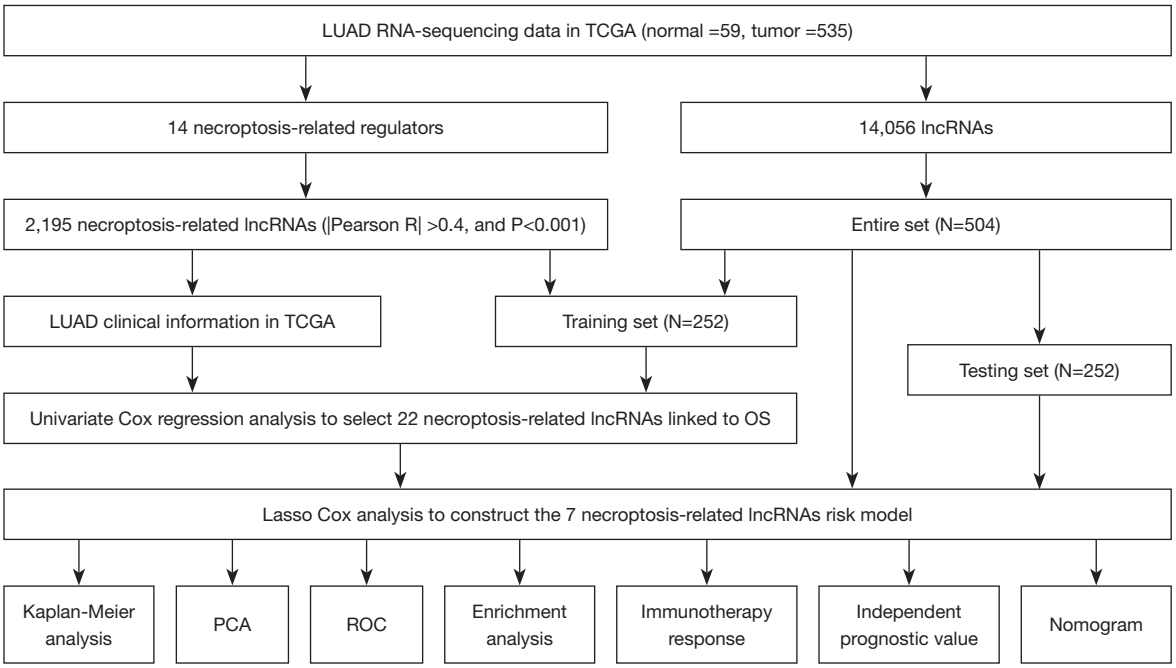

Figure 1 Schematic workflow of the study. LUAD, lung adenocarcinoma; TCGA, The Cancer Genome Atlas; lncRNA, long non-coding RNA; OS, overall survival; PCA, principal component analysis; ROC, receiver operating characteristic.

Principal component analysis (PCA) and Kaplan-Meier (KM) survival analysis

We performed PCA to reduce dimensionality and model identification in both groups for the 14 NRGs, 22 necro-related lncs, and entire gene expression profiles. Finally, we constructed the NecroLncSig based on the expression profiles of the seven necro-related lncs in patients from TCGA. The differences in OS between the two groups were determined by KM survival analysis using the "survminer" and "survival" R packages.

Nomogram and calibration

We constructed a nomogram based on risk score, age, tumor stage, and sex to predict the 1-, 3-, and 5-year OS of patients with LUAD. Next, the Hosmer-Lemeshow test was used to construct the correction curves to determine if the predicted outcomes of the prognostic model were consistent with the actual outcomes.

Investigation of immunotherapy

We used the "maftools" R package to calculate the tumor mutational burden (TMB) based on the tumor-specific mutated genes. Next, we predicted the responses of patients with LUAD to immunotherapy using the Tumor Immune Dysfunction and Exclusion (TIDE) algorithm. The TIDE algorithm captures two key mechanisms of immune evasion: T cell dysfunction and T cell exclusion. A higher TIDE score indicates a greater potential for tumor immune escape and a poorer response to immunotherapy (36).

Statistical analyses

We examined the differences between the two groups using the Student's *t*-test. Next, the OS of the patients was determined by KM survival analysis, and the differences in OS were assessed using the two-sided log-rank test. Finally, the data were statistically analyzed using R version 4.1.1 (https://cran.r-project.org/). P value <0.05 was considered statistically significant.

Results

Identification of necro-related lncs in patients with LUAD

Figure 1 shows the workflow used to construct the NecroLncSig and perform the subsequent analyses. We obtained the samples of 59 healthy subjects and 535 patients

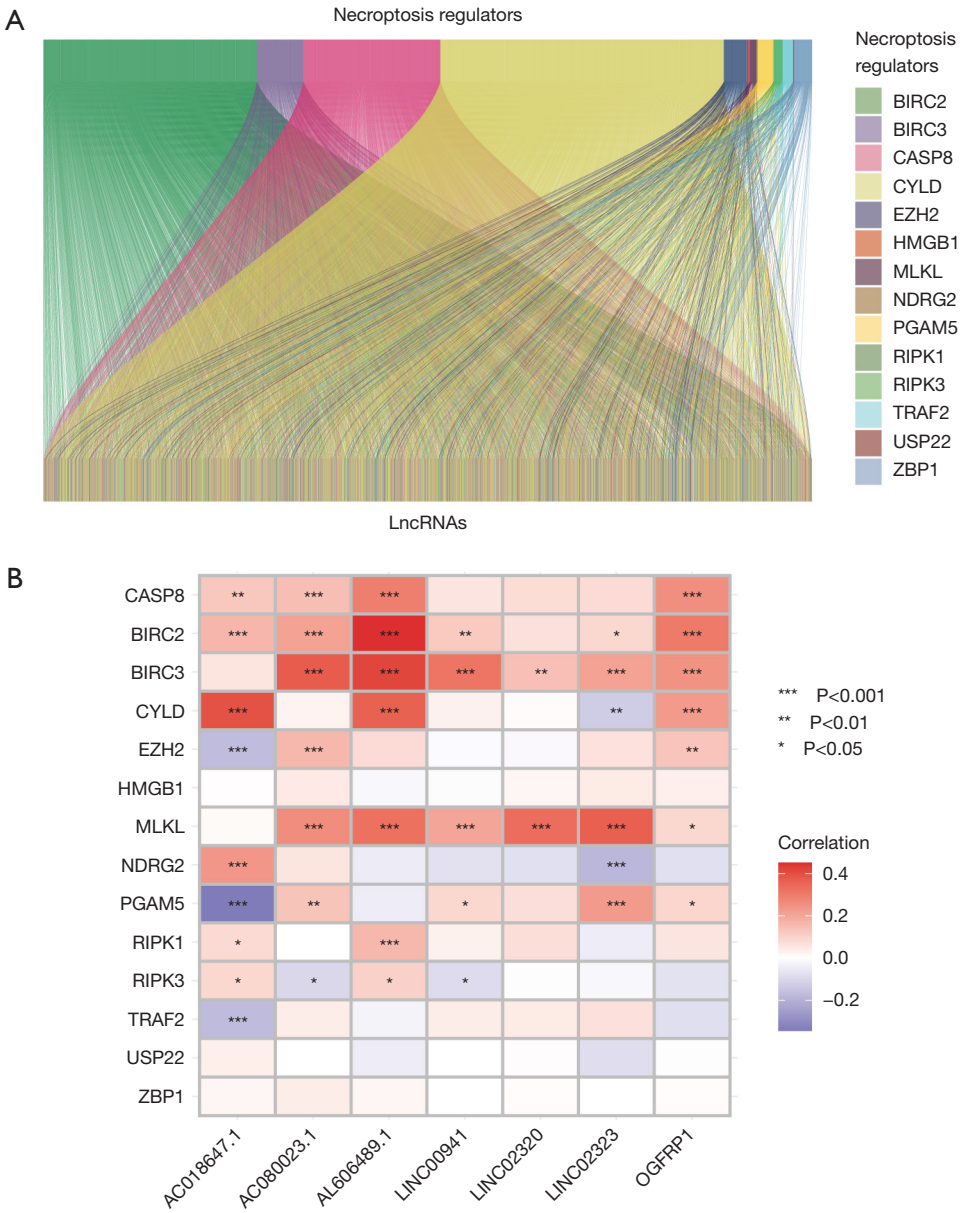

Figure 2 Necro-related lncs in patients with LUAD. (A) The Sankey diagram shows the 14 NRGs and 2,195 necro-related lncs. (B) The heatmap shows the correlation between the 14 NRGs and 7 prognostic necro-related lncs. LncRNA, long non-coding RNA; necro-related lncs, necroptosis-related lncRNAs; LUAD, lung adenocarcinoma; NRGs, necroptosis-related genes.

with LUAD from TCGA. We retrieved the expression profile data of the 14 NRGs and 14,056 lncRNAs using TCGA. The lncRNAs significantly associated with 1 or more of the 14 NRGs (|Pearson R| >0.4 and P<0.001) were considered necro-related lncs. We identified 2,195 necro-related lncs. The necro-related lnc co-expression network is shown in table available at https://cdn.amegroups.cn/static/public/tlcr-24-627-3.xlsx. *Figure 2A* shows the Sankey diagram. *Figure 2B* shows the correlation between the 14 NRGs and the 7 necro-related lncs in the NecroLncSig.

Constructing the NecroLncSig using the training set

The results of univariate Cox regression analysis showed a correlation between 22 of the 2,195 lncRNAs and the OS of the patients in the training set (*Figure 3A*). We

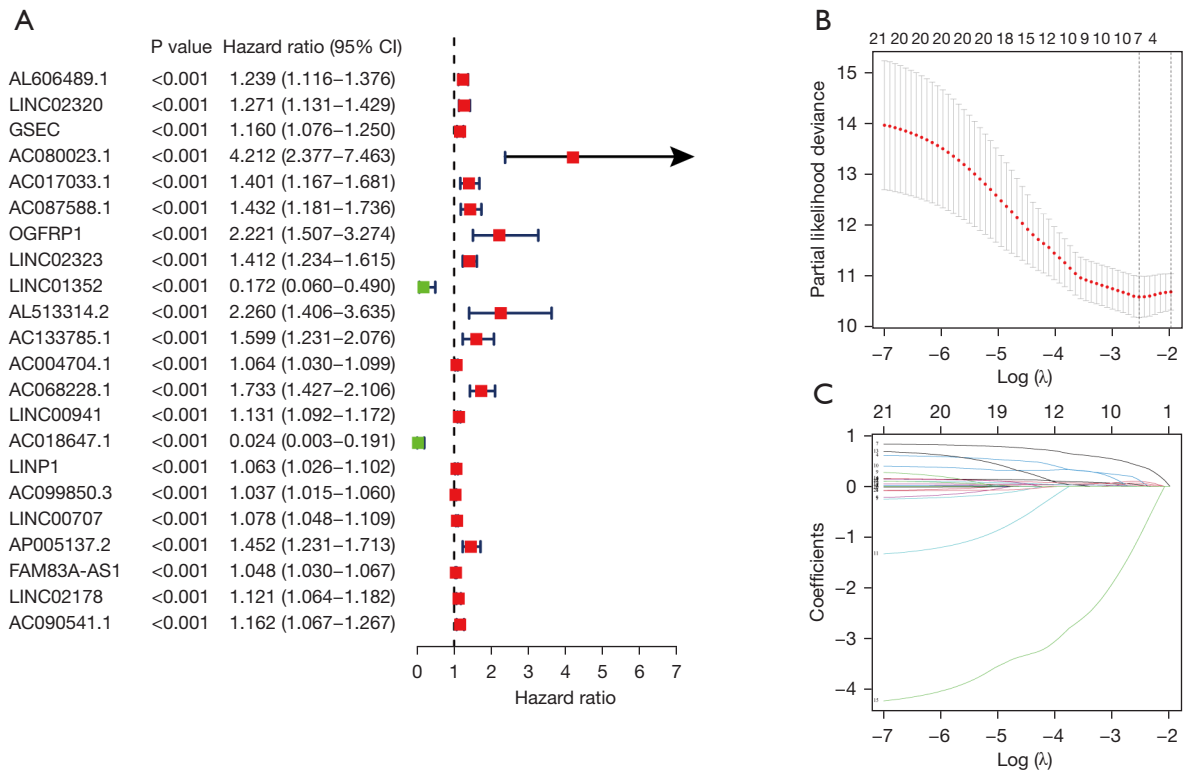

Figure 3 A risk model based on necro-related lncs in patients with LUAD. (A) Necro-related lncs associated with patient prognosis were identified using a univariate Cox regression analysis. (B) The tuning parameters (log λ) of the OS-related proteins were selected to cross-verify the error curve. Perpendicular imaginary lines were drawn at the optimal based on the minimal criterion and 1-se criterion. (C) LASSO coefficient profile of the 22 OS-related lncRNAs. Perpendicular imaginary lines were drawn at the values chosen using 10-fold cross-validation. CI, confidence interval; necro-related lncs, necroptosis-related lncRNAs; lncRNA, long non-coding RNA; LUAD, lung adenocarcinoma; OS, overall survival; 1-se, one standard error; LASSO, least absolute shrinkage and selection operator.

identified seven necro-related lncs (i.e., AL606489.1, LINC02320, AC080023.1, OGFRP1, LINC02323, LINC00941, and AC018647.1) in the training set using LASSO Cox regression analysis. Finally, we constructed the NecroLncSig based on these lncRNAs (*Figure 3B,3C*). The following formula was used to calculate the risk score:

$$\begin{aligned}\text{Risk score} = {} & \text{AL606489.1}\times(0.0349)+\text{LINC02320}\times(0.1001)\\ & +\text{AC080023.1}\times(0.1365)+\text{OGFRP1}\times(0.4084)\\ & +\text{LINC02323}\times(0.0630)+\text{LINC00941}\times(0.0168)\\ & +\text{AC018647.1}\times(-1.0393)\end{aligned} \quad [2]$$

Next, using the median risk score as the threshold, we classified the patients in the training set into the LRG (n=126) and HRG (n=126). The distribution of the risk scores of the patients in the two groups is shown in *Figure 4A*. The survival status and time of patients in the two groups are shown in *Figure 4B*. We observed an increase in expression level of the risk lncRNAs (i.e., AL606489.1, LINC02320, AC080023.1, OGFRP1, LINC02323, and LINC00941), as well as a decrease in the expression level of the protective lncRNA AC018647.1 (*Figure 4C*). Finally, the KM survival curve showed that the OS of patients in the HRG was significantly worse than that of patients in the LRG (P<0.001; *Figure 4D*).

Validating the NecroLncSig

To assess the prognostic significance of NecroLncSig, we calculated the risk scores for patients in both the testing set (n=252) and the entire set (n=504) based on necro-related lnc expression. Patients from the testing set were classified into HRG (n=124) and LRG (n=128), while patients from the entire set were similarly categorized into HRG (n=250)

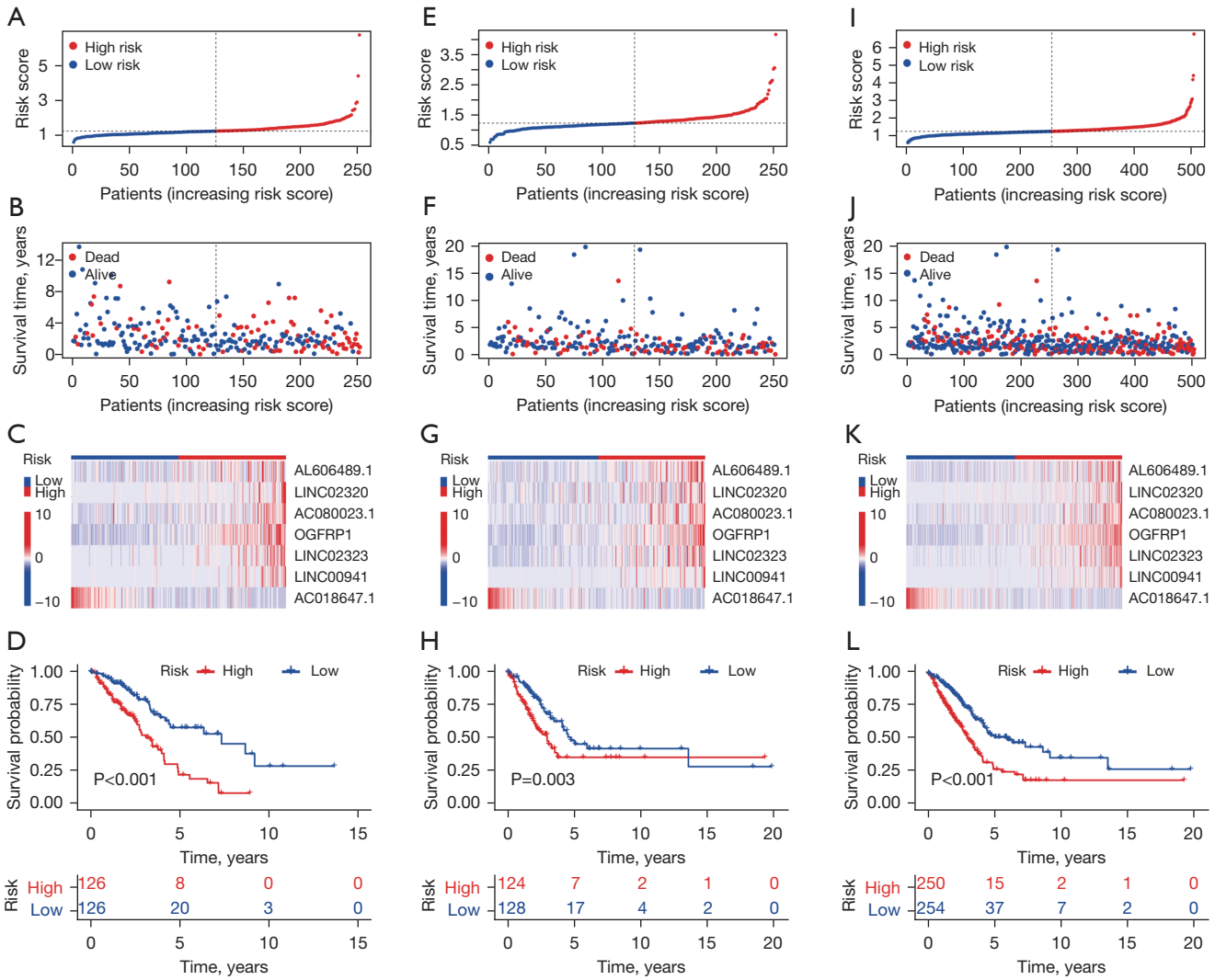

Figure 4 Prognostic significance of the NecroLncSig in the training, testing, and entire sets. (A-L) The distribution, survival status, heatmap of the clustering analysis of the seven necro-related lncs, and KM survival curves of the patients in the HRG and LRG from the (A-D) training, testing (E-H), and entire (I-L) sets. NecroLncSig, necroptosis-related long non-coding RNA signature; necro-related lncs, necroptosis-related lncRNAs; lncRNA, long non-coding RNA; KM, Kaplan-Meier; HRG, high-risk group; LRG, low-risk group.

and LRG (n=254). The distribution of risk scores, necro-related lnc expression levels, survival status, and OSs of patients are depicted in *Figure 4E-4H* for the testing set and *Figure 4I-4L* for the entire set.

Independence of the NecroLncSig and clinical characteristics of LUAD

We performed a stratified analysis to determine if the NecroLncSig could predict the survival of patients with similar clinical characteristics. In the entire set, the patients were classified based on clinical characteristics such as age (≥65/<65 years), sex (female/male), T stage (T1+2/T3+4), N stage (N0+1/N2+3), M stage (M0/M1), and clinical stage (I + II/III + IV). The results demonstrated that the NecroLncSig could classify patients based on age, sex, tumor-node-metastasis, and clinical stage (N0+1, M0, and I + II, respectively) (*Figure 5A-5L*). These results indicate that the NecroLncSig can predict the OS of patients in an independent manner.

Next, univariate and multivariate Cox regression analyses were performed of age, stages, sex, and risk score. The

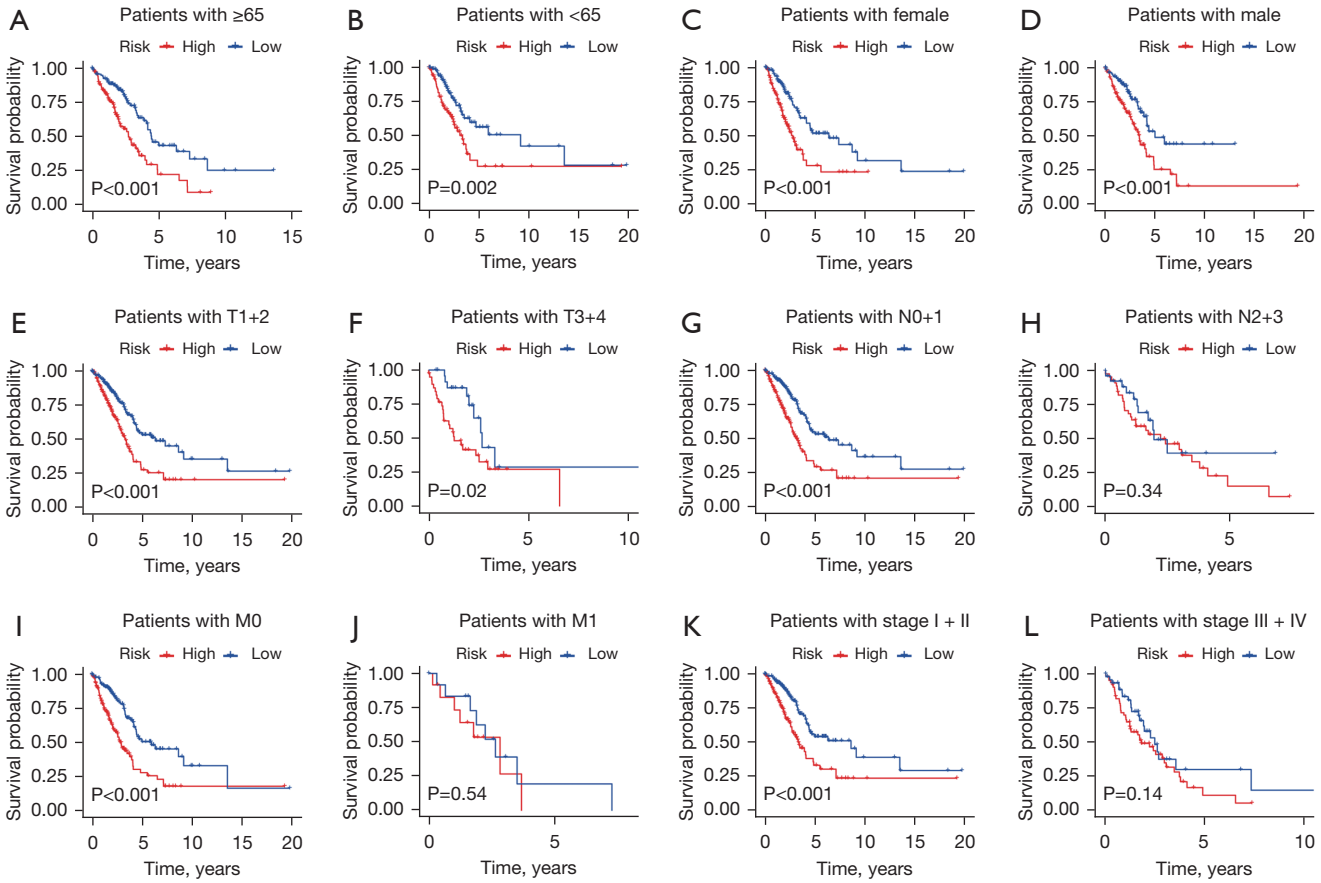

Figure 5 Stratified analysis of the NecroLncSig. (A-L) KM survival curves of the patients in the HRG and LRG in the entire set are classified based on the clinical characteristics of the patients. Age ≥65 years (A), age <65 years (B), female (C), male (D), T1+2 (E), T3+4 (F), N0+1 (G), N2+3 (H), M0 (I), M1 (J), stage I + II (K), and stage III + IV (L). NecroLncSig, necroptosis-related long non-coding RNA signature; KM, Kaplan-Meier; HRG, high-risk group; LRG, low-risk group.

results revealed that the hazard ratio of the risk score was 1.952 [95% confidence interval (CI): 1.652–2.306; P<0.001] (*Figure 6A*) using univariate Cox regression and 1.944 (95% CI: 1.631–2.318; P<0.001) (*Figure 6B* and Table S4) using multivariate Cox regression.

Further, we conducted time-independent ROC curve analysis to determine the sensitivity and specificity of the NecroLncSig in predicting patient prognosis. The conformance index and area under the curve (AUC) values were calculated to assess the risk score. The AUC values of the NecroLncSig for the 1-, 2-, and 3-year OS of the patients were 0.724, 0.739, and 0.725, respectively; in the training set, 0.659, 0.671, and 0.652, respectively, in the testing set; and 0.689, 0.700, and 0.685, respectively, in the entire set (*Figure 6C-6E*). Therefore, the NecroLncSig was able to independently predict patient prognosis with high predictive significance.

PCA

We performed PCA to determine the distribution of the 14 NRGs, 22 necro-related lncs correlated with OS, the entire gene set, and the NecroLncSig (*Figure 7A-7D*) in the patients in the two groups. *Figure 7A-7C* show the scattered distribution of these NRGs, necro-related lncs, the entire gene set, and the NecroLncSig in both the HRG and LRG. The NecroLncSig was able to classify the patients into the HRG and LRG, thereby indicating the significant

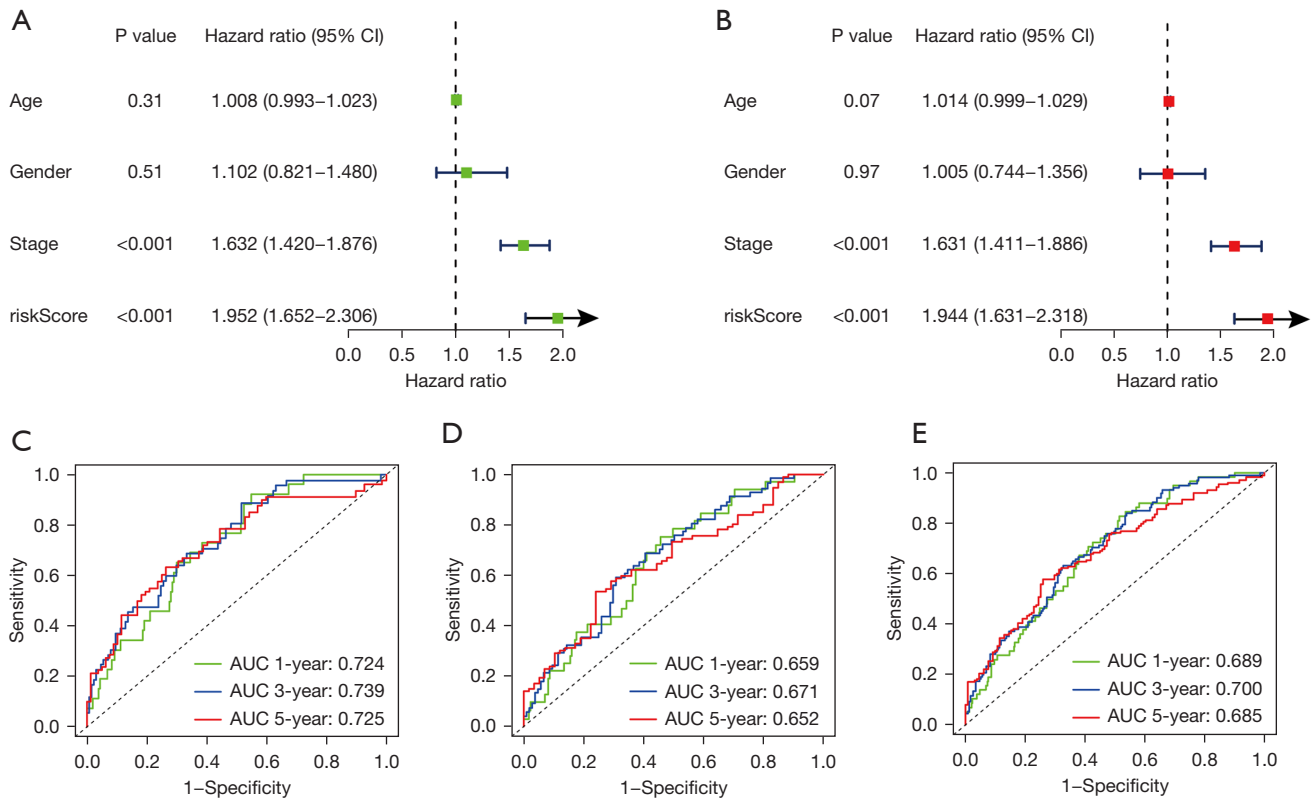

Figure 6 Assessment of the prognostic model developed using necro-related lncs. (A,B) Univariate (A) and multivariate Cox regression analyses (B) of the clinical characteristics and risk score with the OS. (C-E) ROC curves showing the 1-, 3- and 5-year OS of the patients in the training (C), testing (D), and entire (E) sets. CI, confidence interval; AUC, area under the curve; necro-related lncs, necroptosis-related lncRNAs; lncRNA, long non-coding RNA; OS, overall survival; ROC, receiver operating characteristic.

differences between both groups (*Figure 7D*).

GO enrichment analysis and the ability of the NecroLncSig to predict the response of LUAD patients to immunotherapy

We determined the mechanism of the necro-related lncs using GO enrichment analysis. The results demonstrated that the DEGs were primarily enriched in enzyme activity regulation and immune responses (*Figure 8A* and Table S5). In addition, significant differences in the enrichment of terms related to immune responses such as the type_II_interferon response, human leukocyte antigen, parainflammation, and major histocompatibility complex class I, were observed in the HRG and LRG (*Figure 8B*). Furthermore, we examined the correlation between the NecroLncSig and immunotherapy biomarkers. The results revealed that the response of patients in the HRG to immunotherapy was better than that of patients in the LRG, indicating that the NecroLncSig can predict patients' responses to immunotherapy (P<0.05; *Figure 8C*).

Next, we determined the genetic differences between the two groups. *Figure 8D,8E* and table available at https://cdn.amegroups.cn/static/public/tlcr-24-627-4.xlsx show the mutation frequency (92.37) of the patients in the HRG compared to those in the LRG (84.49). A significant difference in *TP53* (50% *vs.* 37%) and titin (45% *vs.* 36%) mutations was observed in the patients in the two groups. In addition, the PD-L1 expression and TMB of patients in the HRG was significantly higher than that of patients in the LRG (P=0.01, *Figure 8F*; P=0.02, *Figure 8G* and table available at https://cdn.amegroups.cn/static/public/tlcr-24-627-5.xlsx).

These results revealed a significant association between

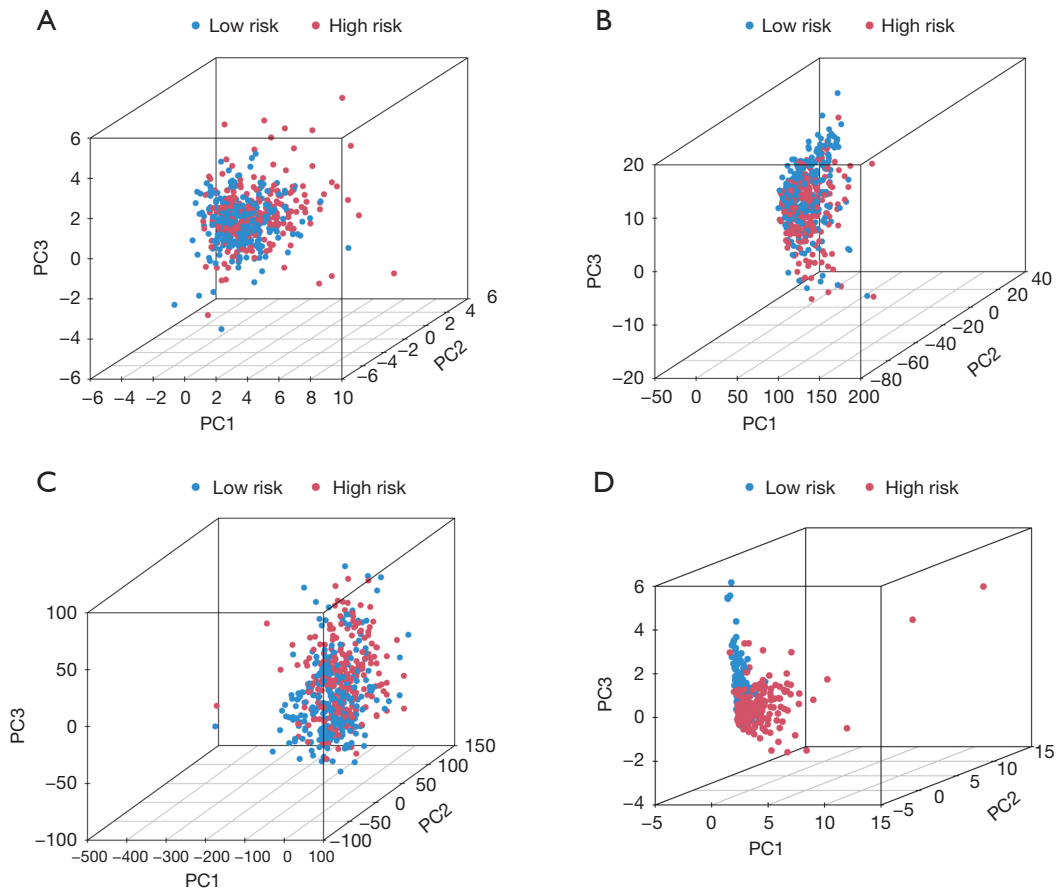

Figure 7 PCA of patients in the HRG and LRG from the entire set. (A-D) PCA based on the 14 NRG expression profiles (A), necro-related lncs (B), entire gene set (C), and seven necro-related lncs used to construct the risk model (D). PC, principal component; PCA, principal component analysis; HRG, high-risk group; LRG, low-risk group; NRG, necroptosis-related gene; necro-related lncs, necroptosis-related lncRNAs; lncRNA, long non-coding RNA.

the TMB and risk scores. Finally, we evaluated the crosstalk between the TMB and risk scores. The survival of patients with a high TMB in the HRG was poor compared to that of patients with a high TMB in the LRG. The survival of patients with a low TMB in the LRG was better than that of patients with a low TMB in the HRG (*Figure 8H*).

Constructing and evaluating nomogram

We constructed the nomogram based on the patients' risk scores and clinical characteristics, including age, tumor stage, and sex, to predict the 1-, 3-, and 5-year OS of the patients (*Figure 9A*). The calibration curves showed that the predicted and the observed OS were consistent (*Figure 9B*).

Discussion

LC is the leading cause of cancer-related deaths worldwide (7,37). Moreover, LUAD is among the most prevalent type of LC in non-smokers (38). Immunotherapy is used to treat patients with advanced non-small cell LC (NSCLC) (39,40). However, only a few patients, specifically those expressing programmed death-ligand 1 levels, benefit from immunotherapy. Necroptosis is a programmed necrotic cell death pathway and regulates the TME and immunotherapy (41). Several studies have used the NecroLncSig to predict patient prognosis (42-45); however, to date, no study has used the NecroLncSig to predict the survival outcomes of patients with LUAD.

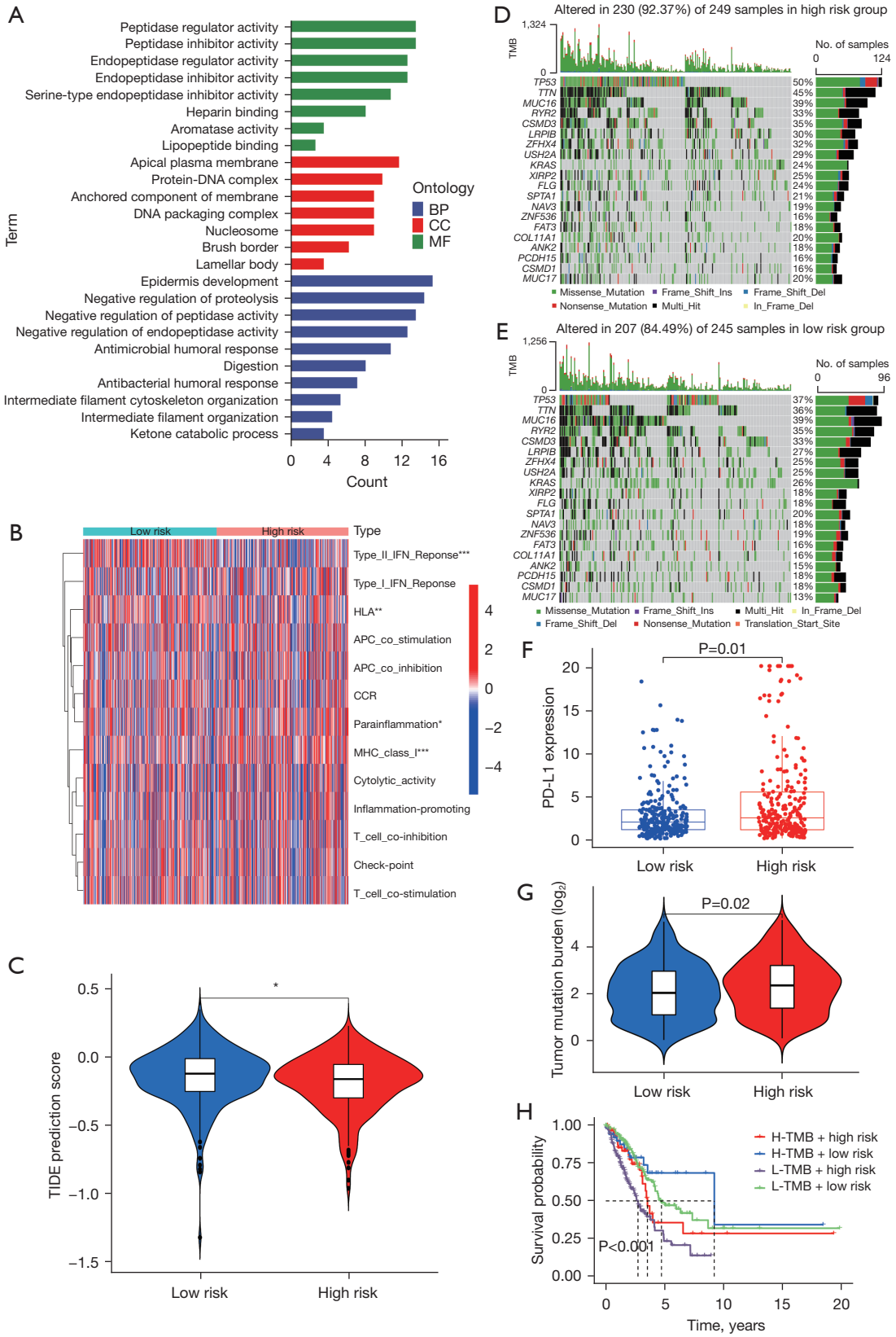

Figure 8 GO enrichment analysis and determining the response of patients to immunotherapy in the entire set using the NecroLncSig.

(A) GO enrichment analysis. (B) Differences in the enrichment of immune-related terms in patients in the HRG and LRG. (C) Differences in the TIDE prediction in patients in the HRG and LRG. (D,E) The waterfall plot shows the gene mutations in patients in the HRG (D) and LRG (E). (F,G) Differences in PD-L1 expression (F) and TMB (G) in patients in the HRG and LRG. (H) KM survival curves show the OS stratified by both the TMB and risk score. *, P<0.05; **, P<0.01; ***, P<0.001. BP, biological progress; CC, cellular component; MF, molecular function; IFN, interferon; HLA, human leukocyte antigen; APC, antigen-presenting cell; CCR, C-C chemokine receptor; MHC, major histocompatibility complex; TIDE, Tumor Immune Dysfunction and Exclusion; TMB, tumor mutational burden; H-TMB, high-TMB; L-TMB, low-TMB; GO, Gene Ontology; NecroLncSig, necroptosis-related long non-coding RNA signature; HRG, high-risk group; LRG, low-risk group; KM, Kaplan-Meier; OS, overall survival.

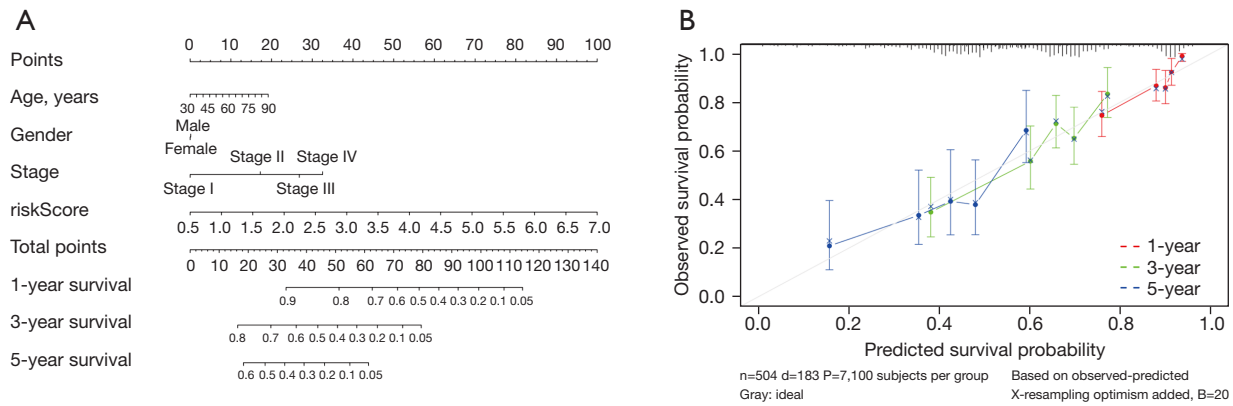

Figure 9 Construction and evaluation of the prognostic nomogram using the entire set. (A) The nomogram based on the age, sex, tumor stage, and risk score could predict the 1-, 3-, and 5-year OS of patients with LUAD. (B) Calibration curves to determine the consistency in the predicted and the actual 1-, 3-, and 5-year OS. OS, overall survival; LUAD, lung adenocarcinoma.

In this study, we constructed the NecroLncSig to predict the prognosis and response of patients with LUAD to immunotherapy. We retrieved 2,195 necro-related lncs from TCGA and examined their ability to predict patient prognosis. We also identified 22 necro-related lncs significantly associated with patient OS. We constructed the NecroLncSig based on seven necro-related lncs (i.e., AL606489.1, LINC02320, AC080023.1, OGFRP1, LINC02323, LINC00941, and AC018647.1). Of these lncRNAs, studies have shown an increase in OGFRP1 expression levels in cancers, including endometrial cancer (46) and cervical carcinoma (47). Further, reduced OGFRP1 expression levels have been shown to attenuate the malignant behavior of endometrial (46), cervical (47), HCC (48), and gestational choriocarcinoma cells (49). LINC02323 regulates the proliferative and migratory abilities of ovarian cancer cells and is associated with transforming growth factor beta in ovarian cancer by targeting miR-1343-3p (50). Moreover, LINC02323 sponges miR-1343-3p to promote the epithelial-mesenchymal transition and metastasis of LUAD cells (51). LINC00941 promotes tumorigenesis and metastasis. An increase in LINC00941 expression promotes the growth and metastasis of HCC, LUAD, and gastric cancer (52-54). This is the first study to identify AL606489.1, LINC02320, AC080023.6, and AC018647.1 as necro-related lncs in LUAD.

We classified the LUAD patients into an HRG and LRG based on the median risk score. The results revealed that the OS of patients in the LRG was higher than that of patients in the HRG. Univariate and multivariate Cox regression analyses showed that the NecroLncSig was able to independently predict patient prognosis. The ROC curve showed that the performance of NecroLncSig in predicting the survival outcomes of patients with LUAD was better than that of conventional clinical characteristics. In addition, the observed *vs.* predicted rates of 1-, 3-, and 5-year OS rates of the nomogram were consistent.

These results demonstrated that the prognostic significance of the NecroLncSig was high. Thus, the

NecroLncSig could serve as a novel biomarker for LUAD.

The TMB is defined as the average number of somatic mutations in the 1 Mb coding region of the genome of tumor cells (55). Studies have reported a correlation between a high TMB and the response of patients to anti-cytotoxic T-lymphocyte-associated protein 4 and programmed cell death protein 1 therapies in NSCLC and uveal melanoma (56-58). This could be due to a higher neo-antigen burden, which could trigger a higher antitumor immune response (56,59,60). Our results showed that the TMB of patients in the HRG was higher than that of patients in the LRG, which suggests that patients in the HRG could benefit from immunotherapy. Moreover, the TIDE results revealed that the response of patients in the HRG to immunotherapy was better than that of patients in the LRG. These results suggest that the NecroLncSig could be a reliable immune biomarker for cancer therapy.

This study has several limitations. First, the retrospective design may introduce inherent biases that could affect our results. Second, our findings have not been validated with independent clinical datasets, which limits the generalizability of the conclusions. Third, the molecular mechanisms underlying the necro-related lncRNAs remain incompletely understood. Lastly, the prognostic model's ability to predict patient outcomes and responses to immunotherapy is currently theoretical. To address these issues, future prospective studies are needed to validate and strengthen these findings.

Conclusions

In conclusion, we constructed a novel NecroLncSig to predict the survival and response of patients to immunotherapy. Our prognostic model could be used to identify patients with LUAD who may respond to immunotherapy with high sensitivity.

Acknowledgments

We would like to thank the staff members of The Cancer Genome Atlas and Gene Expression Omnibus for their involvement in the Cancer Genomics Program. We would also like to thank Bullet Edits Limited for the linguistic editing and proofreading of the manuscript.

Funding: This work was supported by the Medical Science and Technology Foundation of Guangdong Province (No. A2023267) and the Medical and Health Technology Projects of Guangzhou (No. 2015A011086).

Footnote

Reporting Checklist: The authors have completed the TRIPOD reporting checklist. Available at https://tlcr.amegroups.com/article/view/10.21037/tlcr-24-627/rc

Peer Review File: Available at https://tlcr.amegroups.com/article/view/10.21037/tlcr-24-627/prf

Conflicts of Interest: All authors have completed the ICMJE uniform disclosure form (available at https://tlcr.amegroups.com/article/view/10.21037/tlcr-24-627/coif). The authors have no conflicts of interest to declare.

Ethical Statement: The authors are accountable for all aspects of the work in ensuring that questions related to the accuracy or integrity of any part of the work are appropriately investigated and resolved. The study was conducted in accordance with the Declaration of Helsinki (as revised in 2013).

References

1. Bray F, Laversanne M, Sung H, et al. Global cancer statistics 2022: GLOBOCAN estimates of incidence and mortality worldwide for 36 cancers in 185 countries. CA Cancer J Clin 2024;74:229-63.
2. Denisenko TV, Budkevich IN, Zhivotovsky B. Cell death-based treatment of lung adenocarcinoma. Cell Death Dis 2018;9:117.
3. Peters S, Reck M, Smit EF, et al. How to make the best use of immunotherapy as first-line treatment of advanced/metastatic non-small-cell lung cancer. Ann Oncol 2019;30:884-96.
4. Hirsch FR, Suda K, Wiens J, et al. New and emerging

targeted treatments in advanced non-small-cell lung cancer. Lancet 2016;388:1012-24.
5. Saito M, Suzuki H, Kono K, et al. Treatment of lung adenocarcinoma by molecular-targeted therapy and immunotherapy. Surg Today 2018;48:1-8.
6. Li L, Yang L, Cheng S, et al. Lung adenocarcinoma-intrinsic GBE1 signaling inhibits anti-tumor immunity. Mol Cancer 2019;18:108.
7. Hirsch FR, Scagliotti GV, Mulshine JL, et al. Lung cancer: current therapies and new targeted treatments. Lancet 2017;389:299-311.
8. Zhang C, Zhang J, Xu FP, et al. Genomic Landscape and Immune Microenvironment Features of Preinvasive and Early Invasive Lung Adenocarcinoma. J Thorac Oncol 2019;14:1912-23.
9. Cho YS, Challa S, Moquin D, et al. Phosphorylation-driven assembly of the RIP1-RIP3 complex regulates programmed necrosis and virus-induced inflammation. Cell 2009;137:1112-23.
10. Vercammen D, Beyaert R, Denecker G, et al. Inhibition of caspases increases the sensitivity of L929 cells to necrosis mediated by tumor necrosis factor. J Exp Med 1998;187:1477-85.
11. Holler N, Zaru R, Micheau O, et al. Fas triggers an alternative, caspase-8-independent cell death pathway using the kinase RIP as effector molecule. Nat Immunol 2000;1:489-95.
12. Hou J, Ju J, Zhang Z, et al. Discovery of potent necroptosis inhibitors targeting RIPK1 kinase activity for the treatment of inflammatory disorder and cancer metastasis. Cell Death Dis 2019;10:493.
13. Seehawer M, Heinzmann F, D'Artista L, et al. Necroptosis microenvironment directs lineage commitment in liver cancer. Nature 2018;562:69-75.
14. Strilic B, Yang L, Albarrán-Juárez J, et al. Tumour-cell-induced endothelial cell necroptosis via death receptor 6 promotes metastasis. Nature 2016;536:215-8.
15. Höckendorf U, Yabal M, Herold T, et al. RIPK3 Restricts Myeloid Leukemogenesis by Promoting Cell Death and Differentiation of Leukemia Initiating Cells. Cancer Cell 2016;30:75-91.
16. Shi C, Kim T, Steiger S, et al. Crystal Clots as Therapeutic Target in Cholesterol Crystal Embolism. Circ Res 2020;126:e37-52.
17. Najafov A, Chen H, Yuan J. Necroptosis and Cancer. Trends Cancer 2017;3:294-301.
18. Rinn JL, Chang HY. Genome regulation by long noncoding RNAs. Annu Rev Biochem 2012;81:145-66.
19. Holoch D, Moazed D. RNA-mediated epigenetic regulation of gene expression. Nat Rev Genet 2015;16:71-84.
20. Mercer TR, Dinger ME, Mattick JS. Long non-coding RNAs: insights into functions. Nat Rev Genet 2009;10:155-9.
21. Ransohoff JD, Wei Y, Khavari PA. The functions and unique features of long intergenic non-coding RNA. Nat Rev Mol Cell Biol 2018;19:143-57.
22. Khan MR, Wu M, Liu G. Tumor-suppressive or tumor-supportive: For p53, that is the question. Mol Cell Oncol 2018;5:e1408537.
23. Tran DDH, Kessler C, Niehus SE, et al. Myc target gene, long intergenic noncoding RNA, Linc00176 in hepatocellular carcinoma regulates cell cycle and cell survival by titrating tumor suppressor microRNAs. Oncogene 2018;37:75-85.
24. Choi ME, Price DR, Ryter SW, et al. Necroptosis: a crucial pathogenic mediator of human disease. JCI Insight 2019;4:e128834.
25. Malireddi RKS, Kesavardhana S, Kanneganti TD. ZBP1 and TAK1: Master Regulators of NLRP3 Inflammasome/Pyroptosis, Apoptosis, and Necroptosis (PAN-optosis). Front Cell Infect Microbiol 2019;9:406.
26. Cheng M, Lin N, Dong D, et al. PGAM5: A crucial role in mitochondrial dynamics and programmed cell death. Eur J Cell Biol 2021;100:151144.
27. Wen S, Li X, Ling Y, et al. HMGB1-associated necroptosis and Kupffer cells M1 polarization underlies remote liver injury induced by intestinal ischemia/reperfusion in rats. FASEB J 2020;34:4384-402.
28. Zhu J, Yang LK, Wang QH, et al. NDRG2 attenuates ischemia-induced astrocyte necroptosis via the repression of RIPK1. Mol Med Rep 2020;22:3103-10.
29. Lou X, Zhu H, Ning L, et al. EZH2 Regulates Intestinal Inflammation and Necroptosis Through the JNK Signaling Pathway in Intestinal Epithelial Cells. Dig Dis Sci 2019;64:3518-27.
30. Petersen SL, Chen TT, Lawrence DA, et al. TRAF2 is a biologically important necroptosis suppressor. Cell Death Differ 2015;22:1846-57.
31. Roedig J, Kowald L, Juretschke T, et al. USP22 controls necroptosis by regulating receptor-interacting protein kinase 3 ubiquitination. EMBO Rep 2021;22:e50163.
32. Gong Y, Fan Z, Luo G, et al. The role of necroptosis in cancer biology and therapy. Mol Cancer 2019;18:100.
33. Lalaoui N, Lindqvist LM, Sandow JJ, et al. The

molecular relationships between apoptosis, autophagy and necroptosis. Semin Cell Dev Biol 2015;39:63-9.
34. Sarcognato S, Jong IEM, Fabris L, et al. Necroptosis in Cholangiocarcinoma. Cells 2020;9:982.
35. Pasparakis M, Vandenabeele P. Necroptosis and its role in inflammation. Nature 2015;517:311-20.
36. Jiang P, Gu S, Pan D, et al. Signatures of T cell dysfunction and exclusion predict cancer immunotherapy response. Nat Med 2018;24:1550-8.
37. Tan AC, Tan DSW. Targeted Therapies for Lung Cancer Patients With Oncogenic Driver Molecular Alterations. J Clin Oncol 2022;40:611-25.
38. Duma N, Santana-Davila R, Molina JR. Non-Small Cell Lung Cancer: Epidemiology, Screening, Diagnosis, and Treatment. Mayo Clin Proc 2019;94:1623-40.
39. Mazieres J, Drilon A, Lusque A, et al. Immune checkpoint inhibitors for patients with advanced lung cancer and oncogenic driver alterations: results from the IMMUNOTARGET registry. Ann Oncol 2019;30:1321-8.
40. Dafni U, Tsourti Z, Vervita K, et al. Immune checkpoint inhibitors, alone or in combination with chemotherapy, as first-line treatment for advanced non-small cell lung cancer. A systematic review and network meta-analysis. Lung Cancer 2019;134:127-40.
41. Sprooten J, De Wijngaert P, Vanmeerbeerk I, et al. Necroptosis in Immuno-Oncology and Cancer Immunotherapy. Cells 2020;9:1823.
42. Luo L, Li L, Liu L, et al. A Necroptosis-Related lncRNA-Based Signature to Predict Prognosis and Probe Molecular Characteristics of Stomach Adenocarcinoma. Front Genet 2022;13:833928.
43. Liu L, Huang L, Chen W, et al. Comprehensive Analysis of Necroptosis-Related Long Noncoding RNA Immune Infiltration and Prediction of Prognosis in Patients With Colon Cancer. Front Mol Biosci 2022;9:811269.
44. Jiang F, Zhan Z, Yang Y, et al. Construction and Validation of a Necroptosis-Related lncRNA Signature in Prognosis and Immune Microenvironment for Glioma. J Oncol 2022;2022:5681206.
45. Zhang L, Chen Y, Hu W, et al. A novel necroptosis-related long noncoding RNA model for predicting clinical features, immune characteristics, and therapeutic response in clear cell renal cell carcinoma. Front Immunol 2023;14:1230267.
46. Lv Y, Chen S, Wu J, et al. Upregulation of long non-coding RNA OGFRP1 facilitates endometrial cancer by regulating miR-124-3p/SIRT1 axis and by activating PI3K/AKT/GSK-3β pathway. Artif Cells Nanomed Biotechnol 2019;47:2083-90.
47. Zou K, Yu H, Chen X, et al. Silencing long noncoding RNA OGFRP1 inhibits the proliferation and migration of cervical carcinoma cells. Cell Biochem Funct 2019;37:591-7.
48. Chen W, You J, Zheng Q, et al. Downregulation of lncRNA OGFRP1 inhibits hepatocellular carcinoma progression by AKT/mTOR and Wnt/β-catenin signaling pathways. Cancer Manag Res 2018;10:1817-26.
49. Meng Q, Xue H. Knockdown of lncRNA OGFRP1 Inhibits Proliferation and Invasion of JEG-3 Cells Via AKT/mTOR Pathway. Technol Cancer Res Treat 2020;19:1533033820905823.
50. Li Y, Zhao Z, Sun D, et al. Novel long noncoding RNA LINC02323 promotes cell growth and migration of ovarian cancer via TGF-β receptor 1 by miR-1343-3p. J Clin Lab Anal 2021;35:e23651.
51. Zhang X, Du L, Han J, et al. Novel long non-coding RNA LINC02323 promotes epithelial-mesenchymal transition and metastasis via sponging miR-1343-3p in lung adenocarcinoma. Thorac Cancer 2020;11:2506-16.
52. Yan X, Zhang D, Wu W, et al. Mesenchymal Stem Cells Promote Hepatocarcinogenesis via lncRNA-MUF Interaction with ANXA2 and miR-34a. Cancer Res 2017;77:6704-16.
53. Wang L, Zhao H, Xu Y, et al. Systematic identification of lincRNA-based prognostic biomarkers by integrating lincRNA expression and copy number variation in lung adenocarcinoma. Int J Cancer 2019;144:1723-34.
54. Luo C, Tao Y, Zhang Y, et al. Regulatory network analysis of high expressed long non-coding RNA LINC00941 in gastric cancer. Gene 2018;662:103-9.
55. Campbell BB, Light N, Fabrizio D, et al. Comprehensive Analysis of Hypermutation in Human Cancer. Cell 2017;171:1042-1056.e10.
56. Chan TA, Yarchoan M, Jaffee E, et al. Development of tumor mutation burden as an immunotherapy biomarker: utility for the oncology clinic. Ann Oncol 2019;30:44-56.
57. Hellmann MD, Ciuleanu TE, Pluzanski A, et al. Nivolumab plus Ipilimumab in Lung Cancer with a High Tumor Mutational Burden. N Engl J Med 2018;378:2093-104.
58. Van Allen EM, Miao D, Schilling B, et al. Genomic correlates of response to CTLA-4 blockade in metastatic melanoma. Science 2015;350:207-11.
59. Rizvi NA, Hellmann MD, Snyder A, et al. Cancer immunology. Mutational landscape determines sensitivity

to PD-1 blockade in non-small cell lung cancer. Science 2015;348:124-8.
60. Chan TA, Wolchok JD, Snyder A. Genetic Basis for Clinical Response to CTLA-4 Blockade in Melanoma. N Engl J Med 2015;373:1984.

(English Language Editor: L. Huleatt)

Cite this article as: Lin C, Lin K, Lin X, Yuan H, Zhang Y, Xie Z, Dai Y, Liu L, Shimada Y, Goto T, Okuda K, Liu T, Wei C. Necroptosis-related lncRNAs: biomarkers for predicting prognosis and immune response in lung adenocarcinoma. Transl Lung Cancer Res 2024;13(10):2713-2728. doi: 10.21037/tlcr-24-627